The Evolution of Neutron Straw Detector Applications in Homeland Security

Jeffrey L. Lacy, *Member, IEEE*, Athanasios Athanasiades, *Member, IEEE*, Christopher S. Martin, Liang Sun, *Member, IEEE*, and Gerson L. Vazquez-Flores, *Member, IEEE*

***Abstract*—The dwindling supply of ^{3}He has necessitated the adoption of new technologies for detection of neutrons especially in Homeland Security (HS), where detectors require large volumes of the precious gas. The boron-coated straw (BCS) technology consists of very thin-walled metal tubes equipped with a highly robust coating of $^{10}B_4C$ on the inner wall. The coating, applied with Physical Vapor Deposition (PVD), is atomically bound to the metal substrate, and it is able to resist delamination over a temperature range from $-200°C$ to $1000°C$. Accelerated lifetime testing of sealed straw detectors over extreme temperature ranges ($-70°C$ to $+125°C$) have recently demonstrated a 99% expected lifetime of 30 years. At the same time, the coating purity is high, with a ^{10}B content approaching 77%. Straws stacked 5 deep in a dense array have demonstrated an efficiency of $>70\%$ when evaluated in a cold neutron beam. A number of field worthy HS detectors have been developed over the past 2 years based on the BCS. Examples are presented, including neutron modules for Radiation Portal Monitors (RPM), a vehicle mounted modular detector with an intrinsic efficiency of 30% for unmoderated ^{252}Cf neutrons, and handheld detectors. All of these systems have been government tested. The $^{10}B_4C$ coated straw offers a highly versatile, robust and low cost technology meeting multiple needs in homeland and international security.**

***Index Terms*—^{3}He replacement, boron-lined detectors, RPM, handheld detectors, vehicle-mounted detectors.**

I. Introduction

THE boron-coated straw (BCS) detector is a long thin walled tube, coated on the inside with a thin layer of ^{10}B-enriched boron carbide ($^{10}B_4C$). Interior wall coating is achieved by first coating a thin metal foil, using Physical Vapor Deposition (PVD), and then constructing the tube using the coated foil as starting material. Using this methodology, straw diameters can be readily achieved over the range 2 mm up to 15 mm or more.

Because of its construction, an optimal PVD coating technique can be employed providing an unexcelled level of adhesion reliability through atomic bonding and very high purity. The PVD process provides a coating that is chemically pure containing 77% ^{10}B. Conventional boron-lined gas detectors employ chemically applied coatings that compromise robustness and also add undisclosed quantities of binder materials that degrade charged particle escape. PVD deposits $^{10}B_4C$ in very thin and uniform layers, maximizing the fraction of reaction products that escape into the gas. An intrinsic efficiency over 70% has been demonstrated with BCS detectors irradiated in a cold neutron beam at the High Flux Isotope Reactor [1].

Moreover, the robustness of the PVD coating, demonstrated through temperature shock testing carried out over the range $-200°C$ to $1000°C$, makes it feasible to employ low cost foil forming techniques. These techniques have been applied to distort the cylindrical shape of the BCS cathode, providing a larger coated area.

Thermal neutrons captured in ^{10}B are converted into secondary particles, through the ^{10}B(n, α) reaction: $^{10}\mathrm{B} + \mathrm{n} \rightarrow {}^{7}\mathrm{Li} + \alpha$. The ^{7}Li and α particles are emitted isotropically in opposite directions with kinetic energies of 1.47 MeV and 0.84 MeV, respectively. For a boron carbide layer that is 1 μm thick, one of the two charged particles escape the wall 78% of the time, and ionize the gas contained within the straw. Decrease in coating thickness produces a near linear increase in escape efficiency, as shown later in Fig. 5(a).

Each BCS is operated as a proportional detector, with its wall acting as the cathode, and a thin wire tensioned through its center serving as the anode electrode, operated at a high positive potential. Primary electrons liberated in the gas drift to the anode, and in the high electric field close to the anode, avalanche multiplication occurs, delivering a very much amplified charge on the anode wire. Standard charge-sensitive preamplifier and shaping circuitry are used to produce a low noise pulse for each neutron event. Gamma interactions in the wall produce near minimum ionizing electrons that deposit a small fraction of the energy of the heavily ionizing alpha and ^{7}Li products. Gamma signals are effectively discriminated with a simple pulse height threshold.

BCS detectors have design and operational features similar to those of ^{3}He tubes, including the cylindrical electrode geometry, gas ionization and avalanche, and readout with charge-sensitive amplifiers. As a result in most cases the ^{3}He amplifying electronics and high-voltage supplies in existing devices can be completely preserved when ^{3}He tubes are replaced with BCS detectors. Moreover, with close packing, small diameter cylindrical or corrugated BCS detectors can achieve detection efficiency equivalent to that of ^{3}He tubes, 2.54 cm (1 in) in diameter, pressurized to 2.9 atm. Since 2.7 atm is the cutoff for dangerous goods classification, the vast majority of ^{3}He tubes used

Manuscript received June 15, 2012; revised December 04, 2012, January 28, 2013; accepted February 07, 2013. Date of publication March 27, 2013; date of current version April 10, 2013. This work was supported by the U.S. Department of Homeland Security, Domestic Nuclear Detection Office (DNDO), under competitively awarded Contract HSHQDC-11-C-00087. This support does not constitute an expressed or implied endorsement on the part of the Government. This work was additionally supported by the U.S. Defense Threat Reduction Agency (DTRA), under Contract DTRA-01-02-D-0067.

The authors are with Proportional Technologies, Inc., Houston, TX 77054 USA (e-mail: jlacy@proportionaltech.com).

Color versions of one or more of the figures in this paper are available online at http://ieeexplore.ieee.org.

Digital Object Identifier 10.1109/TNS.2013.2248166

in portable devices utilize pressures below this level. Through use of small diameter arrays and corrugation the BCS technology thus offers the potential of providing direct tube replacements for the majority of field applications in which both electronics and physical packaging such as moderator structure can be preserved.

Other neutron detection technologies have been proposed to replace ^{3}He tubes in homeland security applications. They include conventional boron-lined counters (BLCs), like those developed by GE Reuter Stokes [2], [3] and Centronic [4], [5]; scintillating glass fibers loaded with ^{6}Li [6]; wavelength-shifting plastic fibers coated with ^{6}Li/ZnS(Ag), a combination of neutron absorber and scintillator [7]; and BF_3 proportional counters.

Some of these have inherent disadvantages: because BF_3 gas is highly toxic, its applications are severely limited by strict government regulations. Also BF_3 carries limitations as a proportional gas medium that restrict tube pressure to well below 2 atm. Lithium-6-based technologies require the use of photomultiplier tubes (PMTs), light guides, and scintillators components that limit lifetime in the field. In addition, ^{6}Li-based detectors require high speed pulse shape discrimination circuits, to deal with an inherent high sensitivity to gammas. Finally, unlike ^{10}B, which is currently routinely produced in large quantities and plentifully available in free commerce, ^{6}Li enrichment has not been carried out since the closure of Y-12. The processes employed required use of large quantities of mercury [8]. As a result, mercury is a major feature of the contaminated environmental media legacy at Y-12 and other methods must be developed for any future production.

Conventional BLC's have been recently employed in portal monitors and other applications, but suffer from impaired efficiency, resulting from undisclosed levels of binders used in the coating process. As discussed above, and demonstrated later, a thin, pure coating is needed to reach neutron efficiency comparable to that of ^{3}He tubes.

Other neutron detection technologies for potential use in security applications include ^{10}B or Gd-coated microchannel plates (MPCs) [9]; and solid state detectors that employ either 3D silicon pillar arrays filled with ^{10}B [10], or trenches in silicon, backfilled with ^{6}LiF [11]–[16]. These alternatives although attractive for the smallest handheld devices have drawbacks when larger form factors are considered such as replacement of systems that employ 2.54 cm (1-inch) and 5.08 cm (2-inch) ^{3}He tubes of lengths above 10–15 cm. Since these crystal devices employ no charge amplification, very sensitive low noise electronics are required for signal detection. Such electronics can service only limited areas of detector because of capacitive noise effects that are proportional to detector area. Thus, while a wire proportional system or ^{6}Li scintillator with very high absolute efficiency can be readout out with only one electronic channel, a solid state device of similar sensitivity requires hundreds to thousands of parallel counting channels.

We have previously published on the BCS detection capabilities, fabrication, and development of detectors for various applications, including homeland security [17]–[25], neutron science [1], [26]–[30], and nuclear safeguards [31], [32]. Here, we present the design and performance of the latest BCS-based solutions developed to replace ^{3}He tubes in homeland security detectors.

Fig. 1. Portal modules with 30/15 mm straws (left), 60/7.5 mm straws (center), and 95/4.4 mm straws (right).

II. BCS-Based Detectors for Homeland Security

A. Portals

The Domestic Nuclear Detection Office (DNDO) has previously funded Proportional Technologies, Inc. to design, build and test alternative designs for neutron detection modules (NDM) used in radiation portal monitors (RPM). One design developed and tested successfully employed 95 boron-coated straw (BCS) detectors distributed inside a plastic moderator, with dimensions identical to the dimensions of the moderator currently deployed in the vast majority of RPMs. Each BCS was 4.43 mm in diameter and 2 m long. The mean absolute detection efficiency measured among 5 production units was 0.15% (3.5 cps/ng[1]) for a moderated ^{252}Cf source at 2 m, well above the requirement of 0.12%.

In an effort aimed to reduce production cost, associated with the number of BCS detectors employed by the NDM design, a study was carried out to investigate straw diameter effect on response. We selected convenient increments of the original 4.43 mm diameter to 7.5 mm and 15 mm. In order to maintain the same amount of $^{10}B_4C$ coating and hence preserve neutron response, the number of straw detectors was scaled down by a factor of no more than the increase in diameter. Thus, 95/4.43-mm straws contain the same amount of ^{10}B as 56/7.5-mm straws, and 28/15-mm straws.

A 60/7.5-mm straw prototype, populated with 200-cm long straws, and a 30/15-mm straw prototype, populated with 91.4-cm long straws, shown in Fig. 1, have been designed, built and tested. The neutron efficiency of the two prototypes has been measured in outdoor tests, alongside the 95/4.43-mm straw NDM previously delivered to DNDO. The modules were supported vertically against a fence, one at a time, as shown in Fig. 2, and centered 1.1 m, or 1.5 m, above the concrete ground. A moderated or bare source was positioned 2 m away,

[1]The unit of cps/ng is a practical alternative that is commonly used for absolute efficiency, where "cps" denotes the count rate measured in the detector with a source positioned at a specified distance, and "ng" is the ^{252}Cf mass in nanograms; one nanogram of ^{252}Cf emits 2300 neutrons per second.

Fig. 2. NDM testing setup, showing the detector supported against the fence, on the right, and the moderated source supported on a stand, on the left.

TABLE I
NEUTRON EFFICIENCY OF PORTAL NDM DESIGNS

^{252}Cf source at 2 meters	*Absolute Efficiency, % [cps/ng]*		
	95 straws (4.43 mm)	60 straws (7.5 mm)	30 straws[§] (15 mm)
Bare, 1.1 m from ground	0.129% [2.97]	0.132% [3.04]	0.124% [2.84]
Moderated, 1.1 m from ground	0.143% [3.28]	0.144% [3.32]	0.140% [3.21]
Bare, 1.5 m from ground	0.120% [2.76]	0.123% [2.83]	0.116% [2.67]
Moderated, 1.5 m from ground	0.134% [3.07]	0.134% [3.08]	0.130% [2.99]
	Background rate (cps)		
	2.17 cps	2.34 cps	2.54 cps

[§]Results scaled up to correspond to a BCS active length of 200 cm.

centered on the module. The 60/7.5-mm unit was tested also in comprehensive government tests confirming the in house test results reported below. Measurements collected in the 30-straw prototype have been scaled to correspond to an active straw length of 200 cm.

Results are listed in Table I and show that the new designs achieve similar response as the original 95/4.43-mm straw design and all comfortably meet required efficiency. Therefore we conclude that a straw replacement for a single ^{3}He tube RPM system can employ as few as 30 straws of 15 mm diameter. The reduction in straw number by a factor of 3.2 results in a reduction of assembly and testing labor cost by approximately the same factor. Reduction in element number also provides a substantial improvement in manufacturability and maintainability.

Future studies will explore further reduction of straw count through use of corrugated straw structures. If a 2-fold area increase can be achieved for example in a 15 mm design it may be possible to reduce straw number by as much as another factor of 2.

B. Vehicle-Mounted

A vehicle-mounted detection module design is presented in Fig. 3. A total of 309/4.43-mm individually sealed BCS detectors are embedded inside a moderator, as shown in the

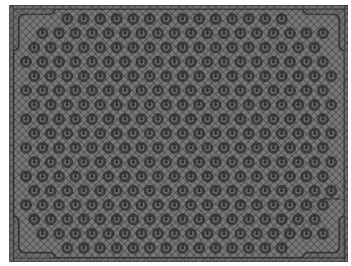

Fig. 3. Cross-section view of 309-straw vehicle-mounted detector.

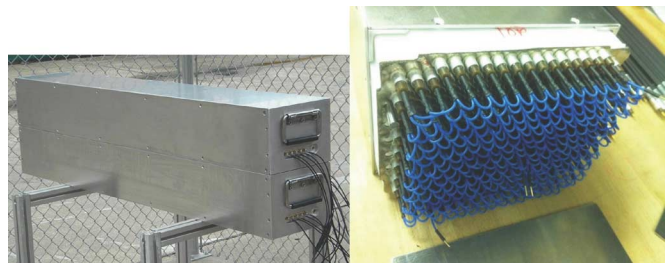

Fig. 4. Prototype neutron detection module.

TABLE II
VEHICLE-MOUNTED DETECTOR PREDICTED AND MEASURED EFFICIENCIES FOR SOURCE AT 2 M

	Predicted	*Measured*
2-module stack		
Absolute efficiency, Unmoderated ^{252}Cf at 2.0 m	0.18% (4.1 cps/ng)	0.18% (4.2 cps/ng)
Intrinsic efficiency, Unmoderated ^{252}Cf	29%	30%

figure. The moderator is composed of a stack of high-density polyethylene (HDPE) segments 5-cm thick each drilled with 309 precision matched holes. The pitch between straw detectors is 1.02 cm. The overall dimensions of the system are 20.3 cm × 15.2 cm × 100 cm (8 in × 6 in × 40 in), and it weighs 20.4 kg (45 lbs). The module can be operated as an independent detector, using simple electronics housed inside the same enclosure as the module itself. Multiple modules can be easily combined to achieve the desired sensitive area and neutron detection efficiency.

A pair of prototype detectors with the above design, pictured in Fig. 4, were fabricated, evaluated and supplied for government testing. During in-house testing, a bare ^{252}Cf source was supported on a stand, 2.0 m away from the detectors, and 1.0 m above the concrete floor. The detectors were also centered 1.0 m above the ground.

The absolute efficiency measured in the 2-module stack was 0.18% (4.2 cps/ng), corresponding to an intrinsic efficiency of 30%. Table II summarizes the measurements.

Monte Carlo Simulations. The detection efficiency of the module pair shown in Fig. 4, was also determined in Monte Carlo simulations implemented in MCNP5. The materials that were simulated included the HDPE moderator, aluminum tubes used to seal the BCS detectors, and the BCS themselves. The latter incorporated a copper wall, adhesive between the copper

layers, and the $^{10}B_4C$ layer. A concrete surface and air were also included, to account for reflections.

The simulated detector pair was oriented with its long axis horizontal, and centered 1 m above a concrete surface. A bare (unmoderated) ^{252}Cf source was simulated at a distance of 2 m from the 30-cm face of the detector pair. A $^{10}B_4C$ layer thickness of 1.0 μm was assumed corresponding to an escape efficiency of 78%, as computed below. The detection efficiency was computed as the product of the neutron interaction rate determined by MCNP5 and the escape efficiency. Both absolute and intrinsic efficiency were determined. The statistical error of values reported below was less than $\pm 1\%$.

The predicted absolute efficiency of the stacked pair of modules was 0.18% (4.1 cps/ng), corresponding to an intrinsic efficiency of 29%. The single module efficiency was 0.078% (1.8 cps/ng). In the 2-module stack, neutrons that thermalize in one module may be detected in the other. As a result, the response of the stack is more than twice that of the single module.

The detection efficiency of the BCS-based module pair was compared against the simulated response of a ^{3}He-based system with moderator outer dimensions 20 cm $\times$ 32 cm $\times$ 87 cm (8 in $\times$ 12.6 in $\times$ 34.25 in), and incorporating 8 ^{3}He tubes, each 5.08 cm in diameter, 86 cm long, and pressurized to 2 atm. The total volume of gas is 28 liters. The MCNP5 simulated neutron efficiency of this module, using the same setup as above (32-cm side irradiated) was 0.14% (3.2 cps/ng), with a corresponding intrinsic efficiency of 27%, slightly lower than the BCS-based module pair, with similar outer dimensions.

Escape efficiency. In order for neutrons stopped in the BCS to be detected, the decay fragments must escape the thin layer of $^{10}B_4C$. The escape probability can be derived analytically from the solid angle formed by the "cone of escape" between the point of neutron interaction and the exit interface [33], and is written as:

$$\varepsilon_{\rm esc} = 1 - {\rm T}/(4{\rm L}_\alpha) - {\rm T}/(4{\rm L}_{\rm Li}), \quad \text{for } {\rm T} \le {\rm L}_{\rm Li} \tag{1a}$$

$$= 0.5 + {\rm L}_{\rm Li}/(4{\rm T}) - {\rm T}/(4{\rm L}_\alpha), \quad \text{for } {\rm L}_{\rm Li} < {\rm T} \le {\rm L}_\alpha \tag{1b}$$

$$= ({\rm L}_\alpha + {\rm L}_{\rm Li})/(4{\rm T}), \quad \text{for } {\rm T} > {\rm L}_\alpha \tag{1c}$$

where T is the film thickness, and L_α and L_{Li} are the ranges of the α and ^{7}Li, respectively, inside the $^{10}B_4C$ film, equal to $L_\alpha = 3.35$ μm and $L_{Li} = 1.69$ μm. The ranges were computed in SRIM-2006.02 [34] for a target layer of $^{10}B_4C$ with a density of 2.38 g/cm^3 and for ion energies of 1.47 MeV for alphas, and 0.84 MeV for ^{7}Li (21% higher energies were used in 6% of all tracks simulated, to account for a corresponding branch of the reaction). Substituting for the ranges in (1), simple relations can be obtained:

$$\varepsilon_{\rm esc} = 1 - 0.223\ {\rm T}, \quad \text{for } {\rm T} \le 1.69 \tag{2a}$$

$$= 0.5 + 0.423/{\rm T} - {\rm T}/13.4, \quad \text{for } 1.69 < {\rm T} \le 3.35 \tag{2b}$$

$$= 1.26/{\rm T}, \quad \text{for } {\rm T} > 3.35 \tag{2c}$$

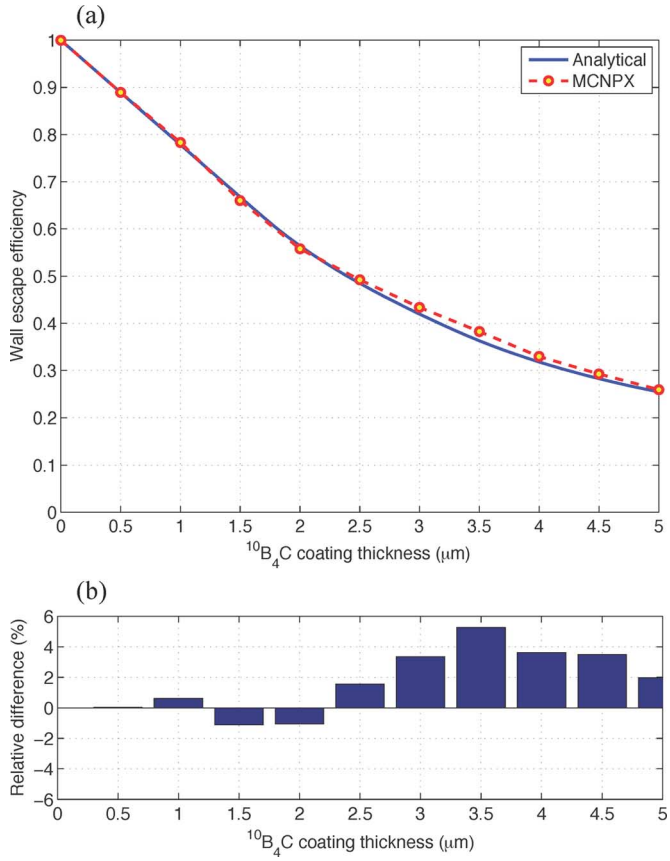

Fig. 5. (a) Combined wall escape efficiency for ^{10}B(n,α) reaction products, as a function of $^{10}B_4C$ coating thickness, and (b) relative difference between the analytical values calculated with (2) and the values obtained with MCNPX.

Equation (2) has been evaluated for T values up to 5 μm, and is plotted in Fig. 5(a). For a $^{10}B_4C$ film thickness of 1.0 μm, the escape efficiency is 78%.

A Monte Carlo simulation, implemented in MCNPX, was completed to confirm the above analysis. The simulation tracked the two reaction products in a thin planar layer of $^{10}B_4C$, and tallied the number escaping one side of the layer. Thermal neutrons were incident normal to the other side of the $^{10}B_4C$ layer, however, it has been verified that the direction of incident neutrons does not affect the escape efficiency in any way, since the reaction products are emitted isotropically, with energies that are many orders of magnitude higher than the neutron energy. The simulation was repeated for different layer thickness, from 0.5 μm to 5.0 μm. The results are plotted in Fig. 5(a), and show very good agreement with (2) in the range $T < 2$ μm, which applies to all detector designs presented in this study. The agreement was comparable to the statistical error ($\pm 1\%$) in the range $T < 2$ μm, and less than 6% in the range up to 5 μm, as plotted in Fig. 5(b).

Equation (2) can therefore be used in place of a full-blown MCNPX simulation that includes tracking of the two reaction products within the coating and other detector materials. Whereas the absorption of neutrons will vary depending on many parameters of the problem (neutron energy and direction, $^{10}B_4C$ coating thickness, number of straws, straw pitch, etc.), the escape of reaction products will only depend on the $^{10}B_4C$

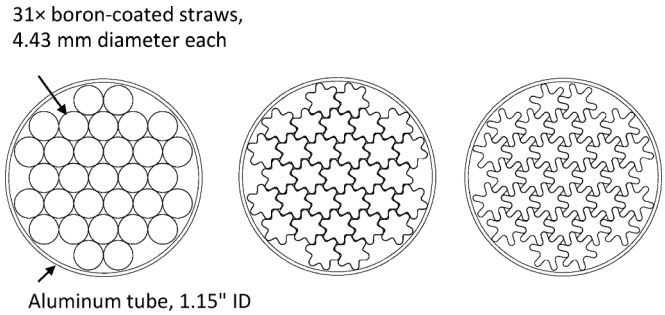

Fig. 6. (Left) Array of 31 boron-coated straws bundled inside a 2.92 cm (1.15in) tube. (middle & right) Design variations with star shaped straws referred to as Star1 (middle) and Star2 (right).

coating thickness, as expressed in (2). It thus makes sense to use an easy-to-implement formula, rather than repeat a component of the Monte Carlo simulation (tracking the reaction products) that will always produce the same result, for a given coating thickness.

C. Handheld

Fig. 6 shows a 31-straw grouping, housed inside a 2.92 cm (1.15 in) aluminum tube. Each straw is 4.43 mm in diameter, and of any desired length. The figure also shows two alternate designs, whereby the round straws have been replaced with star-shaped straws, refered to as Star1 and Star2, in order to increase the boron-coated area by a factor of 1.30 and 1.98, respectively.

Unlike the moderated detector presented earlier, the detection efficiency of a close-packed array of straw detectors can be calculated analytically, assuming a collimated, monoenergetic beam of neutrons incident normally on the side of the array. The analytical formulas offer valuable insight into the design parameters affecting the detection efficiency. They are also easy to implement, and can be used to obtain quick estimates, that can be parameterized. For instance, they can be used to easily obtain the optimal $^{10}B_4C$ coating thickness for any particular detector design. The efficiency ε can be written as:

$$\varepsilon = \varepsilon_{\rm th} \cdot \varepsilon_{\rm esc} \cdot [1 - \exp(-{\rm N}\sigma{\rm t})], \tag{3}$$

where $\varepsilon_{\rm th}$ is the fraction of neutrons counted above the threshold, $\varepsilon_{\rm esc}$ is the wall escape efficiency presented earlier, N is the effective atomic density of ^{10}B in the straw array, σ is the cross section of the ^{10}B(n,α) reaction (3840 barn for thermal neutrons), and t is the array depth in the direction of irradiation (πD/4—for a beam uniformly irradiating the side of a tube with diameter D). The value of N can be calculated as ${\rm N} = {\rm N}_0 \cdot {\rm A_f}$, where ${\rm N}_0 = 1.10 \times 10^{23}$ atoms/cm^3 is the atomic density of ^{10}B in $^{10}B_4C$, and A_f is the fraction of the detector area occupied by the $^{10}B_4C$ coating:

$$A_f = N_s \pi dT / A_0, \tag{4}$$

where N_s is the number of straws (31), d is the straw ID (4.43 mm), T is the coating thickness, and A_0 is the detector cross sectional area ($\pi D^2/4$). In the case of the star-shaped straws, the value of d is substituted by 1.30d or 1.98d, which accounts for the wall area increase for the two shapes, Star1 and Star2, respectively. Using the formulas above, the value of T can be optimized, in order to achieve the maximum possible efficiency in a given detector design.

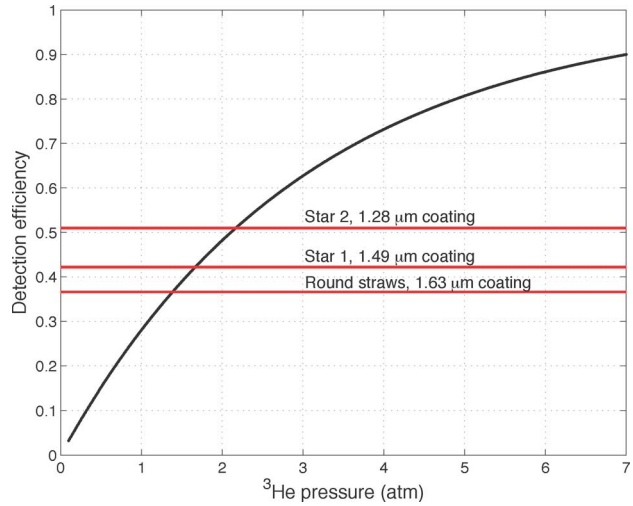

Fig. 7. Intrinsic thermal neutron efficiency of a 2.92 cm (1.15in) ^{3}He tube as a function of gas pressure. The horizontal lines mark the efficiency calculated by (3), for the three BCS detector configurations of Fig. 6.

It is useful to compare the detection efficiency of the BCS array against the detection efficiency of a typical ^{3}He tube. A similar formula applies:

$$\varepsilon_{\rm 3He} = 1 - \exp(-{\rm N_{3He}}\,\sigma_{\rm 3He}{\rm t}) \tag{5}$$

where ${\rm N_{3He}} = 2.69 \times 10^{19} \cdot {\rm P}$ is the atomic density of ^{3}He gas at pressure P, and $\sigma_{\rm 3He}$ is the cross section of the ^{3}He(n,p) reaction (5330 barn for thermal neutrons). The counting efficiency is assumed equal to 1.0, since neutrons convert inside the ^{3}He gas volume, and the released charged particles are fully absorbed. Equation (5) can be solved for the ^{3}He gas pressure that results in an equivalent detection efficiency as the straw-based designs of Fig. 6.

Based on (3), and assuming $\varepsilon_{\rm th} = 0.90$, the intrinsic thermal detection efficiency of the 31-straw design of Fig. 6, populated with round straws, was 36.5%. This same efficiency can be obtained with a 2.92 cm (1.15 in) ^{3}He tube pressurized to 1.38 atm, according to (5), and as shown graphically in Fig. 7. Furthermore, the calculated efficiencies of the Star1 and Star2 designs were 42.1% and 50.9%, respectively, corresponding to equivalent ^{3}He pressures of 1.66 atm and 2.16 atm.

To further establish the equivalency between the 31-straw design and a ^{3}He tube, a Monte Carlo simulation was carried out in MCNP5, in order to determine the response of the two detectors to moderated ^{252}Cf neutrons. The simulated detectors were set up adjacent to a cylindrical moderator that contained the ^{252}Cf source. For the straw detector, the efficiency was obtained as the product of the fraction of neutrons absorbed in ^{10}B (MCNP5), multiplied by the escape efficiency given by (2), and the counting efficiency ($\varepsilon_{\rm th} = 0.90$). Results are summarized in Table III showing that the 31 Star1 straw design, employing an optimal coating of 1.49 μm, has a simulated response equivalent to that of a 1.66 atm 2.92 cm (1.15 in) ^{3}He tube.

A prototype detector, shown in Fig. 8 during construction, was built and tested, employing 31 Star1 straws. The coating thickness in this particular detector was 0.85 μm. The detector response was measured in a laboratory experiment, with a moderated ^{252}Cf source, in a setup identical to the simulation setup described above. The measured absolute efficiency, listed in

TABLE III
NEUTRON ABSOLUTE EFFICIENCY OF STAR1 HANDHELD DETECTOR

	% [cps/ng]	
	Simulated (MCNP5)	Measured
31 Star1 straws, 0.85 μm	0.160 [3.67]	0.154 [3.55]
31 Star1 straws, 1.49 μm	0.189 [4.34]	-
^{3}He tube, 1.66 atm	0.190 [4.37]	-

Fig. 8. Prototype 31 Star1 straw detector during assembly.

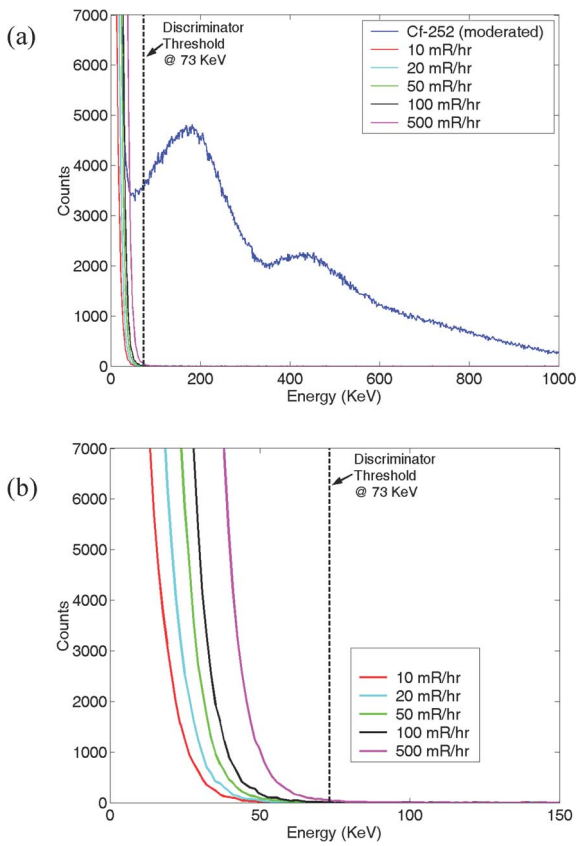

Fig. 9. (a) Pulse height spectra collected in the prototype detector with a moderated ^{252}Cf source, and with a ^{137}Cs source, at the exposure level indicated in the legend. (b) Same as (a) but with a closer view of the gamma tails.

Table III, agrees with the predicted efficiency, within measurement error.

Fig. 9(a) shows the pulse height spectra collected in the detector, over 5 minutes, with the moderated ^{252}Cf source, and with a ^{137}Cs source. The gamma source placement resulted in

TABLE IV
GAMMA INTRINSIC EFFICIENCY OF STAR1 HANDHELD DETECTOR

Gamma exposure rate (mR/hr)	Gammas incident on detector	Gamma counts above threshold	Gamma efficiency
50	2.50×10^{8}	22±7.21	8.79×10^{-8}
100	5.01×10^{8}	36±8.12	7.19×10^{-8}
500	2.50×10^{9}	161±13.8	6.43×10^{-8}

exposure levels of 10, 20, 50, 100 and 500 mR/hr at the detector surface. The figure shows the threshold level used in the measurement of Table III, which successfully discriminates against gamma ray events at very high gamma flux levels (see Fig. 9(b)). Net gamma counts listed in Table IV were collected over a period of 5 minutes. The neutron background rate, measured over a long time period, was 0.1 cps. Exposure rates lower than 50 mR/hr did not yield adequately high net gamma counts for accurate statistics. The gamma efficiencies measured at exposure levels higher than 50 mR/hr were on the order of 10^{-8}, as shown in Table IV.

III. CONCLUSION

The BCS detector systems selected for presentation here serve to illustrate well the high degree of versatility provided by the straw detector basic design. Because coating is applied to the surface of a planar foil, even very narrow foil can be coated in an optimal manner allowing low cost fabrication of even very small round or corrugated structures. These will prove highly beneficial in the smaller direct ^{3}He tube replacement application. In larger diameters, round and corrugated straws can also address well the very largest portal detectors and intermediate vehicle-mounted detectors. The strong electronic similarity of the cylindrical straw detector to that of ^{3}He tubes offers the additional advantage that ^{3}He tubes may be replaced seamlessly while requiring no changes in either electronics or moderator/mechanical systems. A recent article reviewing neutron detectors for the interdiction and verification of special nuclear material (SNM) concludes that "small-diameter, boron-lined proportional tubes" are the most promising technology to replace ^{3}He detectors, in portal monitors and other large-scale applications [35].

The straw neutron detector is a relatively mature ^{3}He replacement technology that offers a cost effective solution that has proven itself compatible with robust and stable operation in field applications. High levels of gamma rejection, matching or exceeding those achieved with ^{3}He, are provided by simple threshold cut that can be adjusted for more or less gamma demanding applications as required (a higher threshold will decrease the neutron detection efficiency).

We have presented here representative detectors addressing the full range of security needs, from small handhelds through the largest portal monitors. We have shown that the number of elements required in the portal monitor application can be very substantially reduced by increasing straw diameter and have presented results for two straw sizes one of which has undergone extensive government testing. Using large numbers of smaller straws (4.43 mm) distributed at a dense pitch of ~1 cm we have shown that a very high performing ^{3}He tube vehicle mounted detector containing 28 liters of ^{3}He in 8 tubes of 5.08 cm (2-inch) diameter can be readily replaced with BCS.

In addition, we have shown that predictions of BCS detection efficiency do not require tracking of ^{10}B(n,α) reaction products inside the $^{10}B_4C$ coating and gas volume. Even though MCNPX can be used to track the alpha and ^{7}Li fragment, simple analytical formulas, given by (2), can successfully predict wall escape probability. The overall BCS detection efficiency then equals the product of the escape probability, and the neutron absorption efficiency obtained in MCNP5.

For the first time we present novel corrugated straw structures that achieve significant increase in Boron coated area while maintaining ease of manufacturing. One of these designs has been prototyped and shown to produce the predicted increase in efficiency while achieving a gamma rejection of 6.4×10^{-8} at a gamma field intensity of 500 mR/hr. Such structures will be explored in future developments concentrating particularly on increased corrugation level with corresponding efficiency benefit. The ultimate objective is to achieve a direct drop-in replacement for bare ^{3}He tubes operating at pressures up to the regulation limit of 2.7 atm.

Future direction will concentrate on low cost production of the basic thin walled round straw element using simple continuous drawing/welding technique. Such forming processes can be readily accomplished following $^{10}B_4C$ coating of raw copper or aluminum foil having a width equal to the desired tube circumference. To accomplish corrugated straw production this thin walled round tubing will be formed either in line or in a secondary process by a second drawing operation. These thin walled detector elements will then be housed in low cost aluminum gas enclosures either as single or multiple tubes.

REFERENCES

[1] J. L. Lacy, L. Sun, A. Athanasiades, C. S. Martin, R. Nguyen, and T. D. Lyons, "Initial performance of large area neutron imager based on boron coated straws," in *Proc. IEEE Nucl. Sci. Conf.*, 2010, pp. 1786–1799.

[2] K. S. McKinny, T. R. Anderson, and N. H. Johnson, "Optimization of coating in boron-10 lined proportional counters," *IEEE Trans. Nucl. Sci.*, to be published.

[3] A. T. Lintereur *et al.*, Boron-Lined Neutron Detector Measurements PNNL report, PNNL-18938, Mar. 7, 2010, (revision 1).

[4] K. Tsorbatzoglou and R. D. McKeag, "Novel and efficient ^{10}B lined tubelet detector as a replacement for ^{3}He neutron proportional counters," *Nucl. Instrum. Meth. A*, vol. 652, no. 1, pp. 381–383, 2011.

[5] M. L. Woodring, J. H. Ely, R. T. Kouzes, and D. C. Stromswold, Boron-Lined Multitube Neutron Proportional Counter Test PNNL report, PNNL-19726, Sept. 6, 2010.

[6] R. S. Seymour *et al.*, "Scintillating-glass-fiber neutron sensors, their application and performance for plutonium detection and monitoring," *J. Radioanalytical and Nuclear Chemistry*, vol. 243, no. 2, pp. 387–388, 2000.

[7] R. T. Kouzes *et al.*, Full Scale Coated Fiber Neutron Detector Measurements PNNL report, PNNL-19264, Mar. 17, 2010.

[8] US Department of Energy, Office of Environmental Management, Linking Legacies: Connecting the Cold War Nuclear Weapons Production Processes to Their Environmental Consequences DOE report DOE/EM-0319, 1997.

[9] W. B. Feller *et al.*, "Microchannel plate special nuclear materials sensor," *Nucl. Instrum. Meth. A*, vol. 652, pp. 25–28, 2011.

[10] R. J. Nikolic *et al.*, "6:1 aspect ratio silicon pillar based thermal neutron detector filled with ^{10}B," *Appl. Phys. Lett.*, vol. 93, p. 133502, 2008.

[11] S. L. Bellinger, R. G. Fronk, W. J. McNeil, T. J. Sobering, and D. S. McGregor, "Enhanced variant designs and characteristics of the microstructured solid-state neutron detector," *Nucl. Instrum. Meth. A*, vol. 652, pp. 387–391, 2011.

[12] D. S. McGregor and J. K. Shultis, "Reporting detection efficiency for semiconductor neutron detectors: A need for a standard," *Nucl. Instrum. Meth. A*, vol. 632, pp. 167–174, 2011.

[13] C. J. Solomon, J. K. Shultis, and D. S. McGregor, "Reduced efficiency variation in perforated neutron detectors with sinusoidal trench design," *Nucl. Instrum. Meth. A*, vol. 618, pp. 260–265, 2010.

[14] D. S. McGregor, W. J. McNeil, S. L. Bellinger, T. C. Unruh, and J. K. Shultis, "Microstructured semiconductor neutron detectors," *Nucl. Instrum. Meth. A*, vol. 608, pp. 125–131, 2009.

[15] J. K. Shultis and D. S. McGregor, "Design and performance considerations for perforated semiconductor thermal-neutron detectors," *Nucl. Instrum. Meth. A*, vol. 606, pp. 608–636, 2009.

[16] W. J. McNeil *et al.*, "1-D array of perforated diode neutron detectors," *Nucl. Instrum. Meth. A*, vol. 604, pp. 127–129, 2009.

[17] J. L. Lacy, A. Athanasiades, C. S. Martin, L. Sun, and G. J. Vazquez-Flores, "Boron-coated straw detectors for backpack monitors," *IEEE Transaction on Nuclear Science*, Jun. 2012, submitted for publication.

[18] J. L. Lacy *et al.*, "Boron-coated straws as a replacement for ^{3}He-based neutron detectors," *Nuclear Instruments and Methods in Physics Research A*, vol. 652, pp. 359–363, 2011.

[19] J. L. Lacy, A. Athanasiades, C. S. Martin, L. Sun, and G. J. Vazquez-Flores, "Straw-based portal monitor ^{3}He replacement detector with expanded capabilities," in *Proc. IEEE Nucl. Sci. Conf.*, Oct. 23–29, 2011, pp. 4865–4868.

[20] J. L. Lacy, A. Athanasiades, C. S. Martin, L. Sun, and G. J. Vazquez-Flores, "Replacement of ^{3}He in constrained-volume homeland security detectors," in *Proc. IEEE Nucl. Sci. Conf.*, Oct. 23–29, 2011, pp. 324–325.

[21] J. L. Lacy, A. Athanasiades, C. S. Martin, L. Sun, G. J. Vazquez-Flores, and T. D. Lyons, "Boron-coated straw detectors: A novel approach for helium-3 neutron detector replacement," in *Proc. IEEE Nucl. Sci. Conf.*, 2010, pp. 3971–3975.

[22] J. L. Lacy, A. Athanasiades, L. Sun, C. S. Martin, and G. J. Vazquez-Flores, "Boron coated straw detectors as a replacement for ^{3}He," in *Proc. IEEE Nucl. Sci. Conf.*, 2009, pp. 119–125.

[23] J. L. Lacy, A. Athanasiades, C. S. Martin, L. Sun, and T. D. Lyons, "Fabrication and materials for a long range neutron-gamma monitor using straw detectors," in *Proc. IEEE Nucl. Sci. Conf.*, 2008, pp. 686–691.

[24] J. L. Lacy, A. Athanasiades, C. S. Martin, L. Sun, J. W. Anderson, and T. D. Lyons, "Long range neutron-gamma point source detection and imaging using unique rotating detector," in *Proc. IEEE Nucl. Sci. Conf.*, 2007, vol. 1, pp. 185–191.

[25] A. Athanasiades *et al.*, "High sensitivity portable neutron detector for fissile materials," in *Proc. IEEE Nucl. Sci. Conf.*, 2005, vol. 2, pp. 1009–1013.

[26] J. L. Lacy, L. Sun, C. S. Martin, R. Nguyen, A. Athanasiades, and Z. Sobolewski, "Initial performance of sealed straw modules for large area neutron science detectors," in *Proc. IEEE Nucl. Sci. Conf.*, Oct. 23–29, 2011, pp. 431–435.

[27] J. L. Lacy, L. Sun, C. S. Martin, A. Athanasiades, and T. D. Lyons, "One meter square high rate neutron imaging panel based on boron straws," in *Proc. IEEE Nucl. Sci. Conf.*, 2009, pp. 1117–1121.

[28] J. L. Lacy, A. Athanasiades, N. N. Shehad, C. S. Martin, and L. Sun, "Performance of 1 meter straw detector for high rate neutron imaging," in *Proc. IEEE Nucl. Sci. Conf.*, 2006, vol. 1, pp. 20–26.

[29] A. Athanasiades, N. N. Shehad, C. S. Martin, L. Sun, and J. L. Lacy, "Straw detector for high rate, high resolution neutron imaging," in *Proc. IEEE Nucl. Sci. Conf.*, 2005, vol. 2, pp. 623–627.

[30] J. L. Lacy, A. Athanasiades, N. N. Shehad, R. A. Austin, and C. S. Martin, "Novel neutron detector for high rate imaging applications," in *Proc. IEEE Nucl. Sci. Conf.*, 2002, vol. 1, pp. 392–396.

[31] J. L. Lacy, A. Athanasiades, C. S. Martin, L. Sun, and G. J. Vazquez-Flores, "Design and performance of high-efficiency counters based on boron-lined straw detectors," 2012 Institute of Nuclear Material Management 2012.

[32] J. L. Lacy, A. Athanasiades, L. Sun, C. S. Martin, G. J. Vazquez-Flores, and S. Mukhopadhyay, "Performance of a straw-based portable neutron coincidence/multiplicity counter," in *Proc. IEEE Nucl. Sci. Conf.*, Oct. 23–29, 2011, pp. 529–532.

[33] D. S. McGrefor, M. D. Hammig, Y.-H. Yang, H. K. Gersch, and R. T. Klann, "Design considerations for thin film coated semiconductor thermal neutron detectors—I: Basics regarding alpha particle emittingneutronreactivefilms," *Nucl. Instrum. Meth. A*, vol. 500, pp. 272–308, 2003.

[34] J. F. Ziegler, M. D. Ziegler, and J. P. Biersack, "SRIM—The stopping and range of ions in matter (2010)," *Nucl. Instrum. Meth. Phys. Res. B*, vol. 268, pp. 1818–1823, 2010.

[35] R. C. Runkle, A. Bernstein, and P. E. Vanier, "Securing special nuclear material: Recent advances in neutron detection and their role in nonproliferation," *J. Appl. Phys.*, vol. 108, p. 111101, 2010.